INVESTIGATION ON THE FAILURE MECHANISMS OF COMPOSITE FASTENERS WITH COUNTERSUNK HEAD IN QUASISTATIC AND FATIGUE LOADING

M. Schuett[1]*, H. Wittich[1], C. Vernier[2], F. Nussbaeumer[2], K. Schulte[1]
[1] Institute of Polymers and Composites, Hamburg University of Technology, Hamburg, Germany, [2] Bishop GmbH Aeronautical Engineers, Hamburg, Germany,
* Corresponding author (martin.schuett@tuhh.de)

Keywords: *Composite bolted joints, Countersunk head CFRP-fasteners, fractography*

1 Introduction

In aircraft industry bolts – made of steel or titanium – are widely used in order to join CFRP structures. They are removable and permit to gain access to the interior of the structure for inspection or repair purposes.
However, the holes in the structural components lead to a stress concentration and the large number of fasteners results in a weight penalty. Additionally the difference in the electrical potential conductivity between the composite laminate and the metallic bolts results in a problem of galvanic corrosion [1, 2]. In order to overcome weight and corrosion problems of the metal fasteners, the idea of using fasteners made of composite materials arose.
In the literature only little information can be found on this type of fasteners. R. Starikov and J. Schön studied the quasi static and fatigue behaviour of titanium and composite fasteners [2, 3]. They found that titanium fasteners perform better than CFRP quasi-statically, but they lose their strength much faster under fatigue: at 10^6 cycles, composite and titanium fasteners fail at the same maximum stress level.
Reworked designs and production process of the CFRP fasteners in the recent years, suggest that the composite fastener has improved [10]. This leads to a much wider field of application. Therefore a deeper understanding of the failure mechanisms in static and fatigue loading is essential. Detailed investigations on composite bolted joints, describe their failure processes in response to several key features such as clamping force, coefficient of friction, clearance/fitting tolerance, joint geometric details and laminate lay-up [4, 6, 7]. In addition, secondary bending in a single lap joint and bending of the bolt create a non-uniform contact stress distribution between the bolt and the hole edge. This results in a shear and tension force on the bolts [1, 2, 7, 8 and 9].
For composite bolted joints four basic failure modes can be observed: net-section failure, bearing, shear out and bolt failure.
The literature overview has shown that the failure process for composite bolted joints with steel or titanium fastener system is described in detail [2-9].
Based on these research results quasi-static test with single lap shear specimens are performed to describe the failure mechanisms of the CFRP-fasteners in detail.

2 Experimental methods

2.1 Materials and Geometry

Single lap shear (SLS), based on ASTM D 7248, are performed using one or two bolts [11].
The composite plates are manufactured from carbon fibre/epoxy material system (T800S-M21) with quasi-isotropic layup $[45/90/-45/0]_{2S}$. The nominal ply thickness is 0.19 mm. The thickness of the CFRP-laminate is h = 3.04 mm. The geometries for the two specimen configurations follow the ASTM D 7248 (Fig. 1). The dimensions of the specimens are related to the diameter *d* of the bolt. For the experiments the nominal shank diameter is d = 4.8 mm. The width of the test specimens is set to w = 30 mm.
Jaws clamp the test specimen at its ends and apply the tensile load. Taps ensure an optimal load transmission into the specimens from the clamping system. A doubler to each grip avoids eccentric loading. The holes in the test specimens are drilled with countersink drillers from the company Klenk. A patented fibre cracker on the drilling tool and

distinct drilling parameters are taken, to minimize delamination, chip-out fibres and degradation of matrix due to overheating in the bore edge [1].

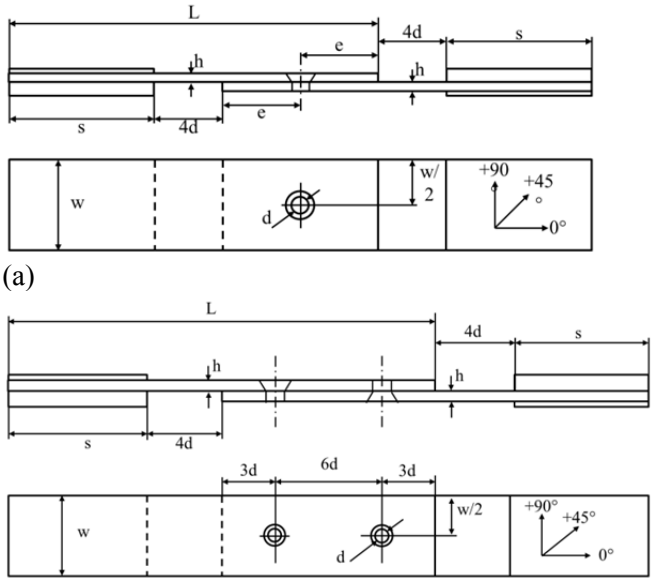

Fig. 1: Specimen geometry for (a) one bolt or (b) two bolts, all dimensions are in millimetre [mm].

In this work two fastener-systems are tested:

- Titanium-bolt (Ti-6Al-4V) and steel-nut (302HQ) aerospace series with countersunk head, shank diameter d = 4.8 mm
- CFRP-bolt (IM7/Peek) with countersunk head, shank diameter d = 4.8 mm, manufactured in close collaboration with the Swiss company IcoTec (Fig. 2)

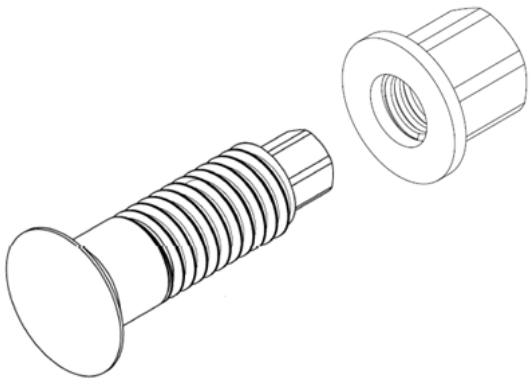

Fig. 2: Sketch of the CFRP-bolt with d = 4.8 mm

Each specimen is mounted either with one or two fasteners. The torque applied to the fasteners was chosen to 5 Nm for these experimental batches.

2.2 Testing procedure

The specimens were loaded in tension using a Zwick Roller Z100 testing machine at a constant cross-head speed of 1mm/min. All experiments were performed at room temperature (≈22°C) and ambient relative humidity.
During the tensile test the global elongation of the specimens, the bending and the elongation of the bolts are plotted.
In order to characterize the failure process of the CFRP-bolt, acoustic emission (AE) is recorded. R. Gutkin et al. point out that peaks in the AE curve of a CFRP-laminate under load correspond to the occurrence of damage [7]. Consequently, tests are stopped and scans of the microstructure are analysed for each peak in order to characterize the evolution of the failure process until breaking.

2.3 Experimental measurement set-up

To monitor the SLS tension tests a number of different measuring systems is in use. The global elongation of the specimen is measured with a Multisence extensometer (Zwick Roller). The initial gage length is given with l_0 = 80 mm.
For all the experiments, a high resolution camera monitors the plate and bolt movement. A Matlab script evaluates the angle change of a plate with respect to the other, as well as the bolt angle relative to its starting position.
For the specimen with two fasteners two strain gauges with 6 mm gauge length, placed on the bolts and between the bore holes, measure the strain distribution and the load transfer between the two bolts. The strain gauges (Typ CEA-06240UZ-120) from the company Vishay were glued on each side of the joint, as shown in Fig. 3.
To detect the AE-signals a simple set-up is used consisting of a microphone BelCat EGT-300 that is placed on the head of the bolt, as shown in Fig. 3. The sensor operates at 44.1 kHz. The detected signal is amplified by 20 dB and recorded via a PC with a 32 bit Soundcard. The AE investigation relies on the principle that events of certain failure modes create a defined acoustic event or acoustic signal.
Furth more an extensometer from the company Sander monitors the elongation of the bolt during a quasistatic tension test of the SLS-specimens. The

extensometer is placed on small metallic index arms which are glued according to Fig. 3 to a bolt.

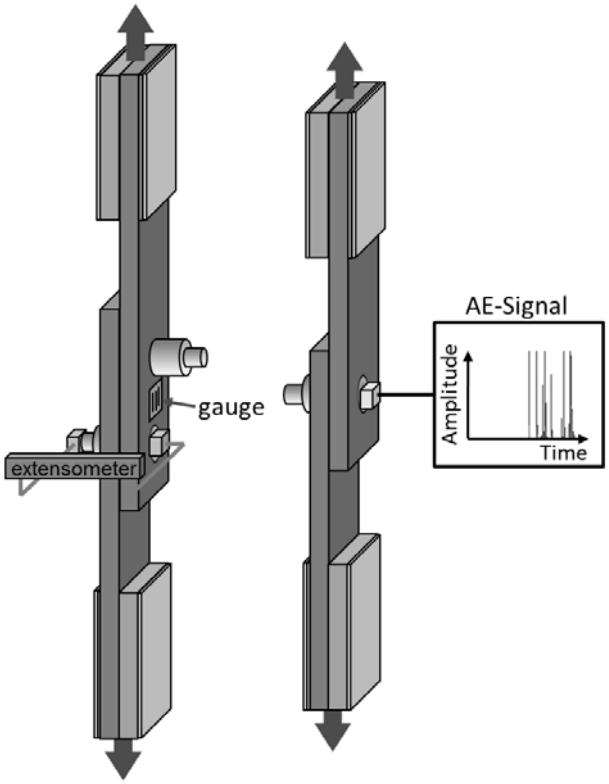

Fig. 3: Specimen geometry for (a) one bolt or (b) two bolts with possible measurement setups of the SLS-specimens with strain gauges, AE-setup and extensometer

For a further inspection of the failure modes light microscopy scans are performed. For this purpose the cross-section of the in tension loaded SLS specimens are polished.

3 Results and Discussion

Quasi-static tensile tests of SLS-specimens with either titanium or CFRP fastener are performed. Each test can be plotted in Bearing Stress/Bearing Strain diagrams. The bearing stress is calculated by the quotient of the normalized applied load divided by the diameter multiplied with the thickness of the plate. Whereas the bearing strain is the normalized hole deformation of the specimen, which is equal to the deformation of the bearing hole in direction of the loading divided by the diameter of the hole.

Comparing the results of SLS-Tests with joints by titanium fasteners and CFRP-fasteners, it is seen that titanium fasteners bear nearly twice the load than the new designed CFRP-fasteners (Fig. 4). Also the slope of the bearing stress/strain curves indicates that the bearing chord stiffness E^{br} for the specimens with CFRP-bolts is 2/3 from the specimens with Ti-bolts. Final failure was considered when the specimen couldn't withstand any further load. The final failure of each specimen was due to failure of the bolt, independent of the bolt material. In comparison the CFRP-bolt fails at lower deformations of the total specimen. The bearing strain ε^{br} of a specimen mounted with CFRP-fasteners is half of the achievable bearing strain for the joints with Ti-bolts.

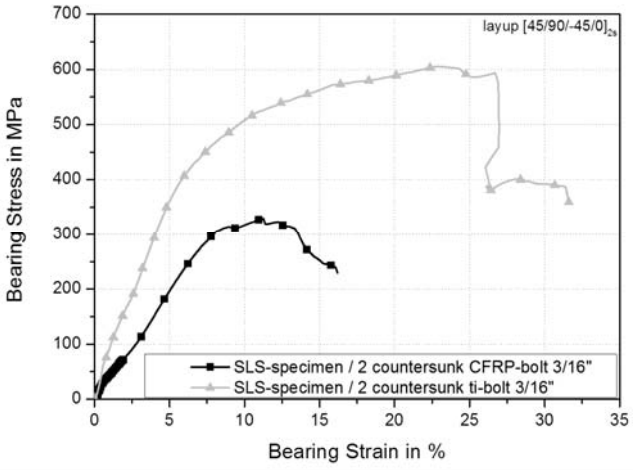

Fig. 4: Comparison of SLS-specimens with a quasi-isotropic layup with either two Ti-bolts or two CFRP-bolts in a Bearing Stress - Bearing Strain diagram

The obtained images of the performed quasi-static SLS-tests for specimens with either one or two CFRP-bolts are displayed in Fig 5. The picture (a) and (d) are the starting positions for the two specimen configurations respectively. In Fig. 5 (b) the maximum attainable relative angle between the two specimen plates for on CFRP-fastener is shown. The left laminate plate, which induces the force of the top clamps into the joint, is marked with the blue line. An investigation of the pictures, show no detectable change of the plate angle with the used camera resolution. Fig. 5 (c) shows the maximum angle of the CFRP-bolt due to the induced forces.

For the specimen configurations with two CFRP countersunk fasteners the maximum plate and bolt angle are shown the Fig 5. (e) and (f). Here a closer look is taken on the lower part of the specimen. The picture (e) displays the maximum angle between the laminate plates at the lower part of the specimen.

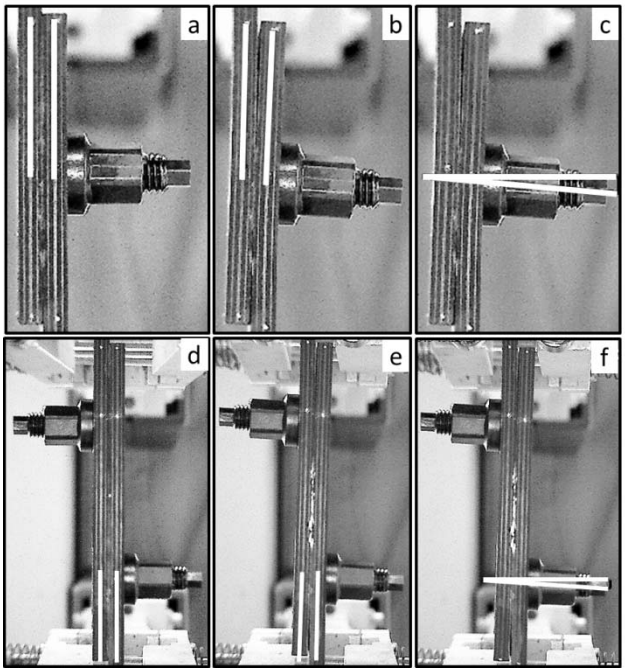

Fig. 5: Monitored plate angle and bolt angle for a SLS-test with one and two CFRP-bolts: (a) starting position, (b) maximum plate angle, (c) maximum bolt angle, (d) starting position, (e) maximum plate angle, (f) maximum bolt angle

Plotting the calculate bolt and plate angles for a SLS-test against the bearing strain, the diagrams in Fig. 6 for a test-specimen with one and in Fig. 7 for two CFRP-fasteners are obtained.
In both diagrams a nearly static increase for either the bolt angle or the laminate plate angle can be detected. For both specimen configurations the maximum plotted angle corresponds to a bearing strain of 10%. At this point the bolts failed due to a shear failure of the countersunk head of the CFRP-bolts.
The maximum plate angle for a specimen with one fastener is by more than 1° higher than for a test specimen with two CFRP-bolts (Fig. 6 and Fig. 7)

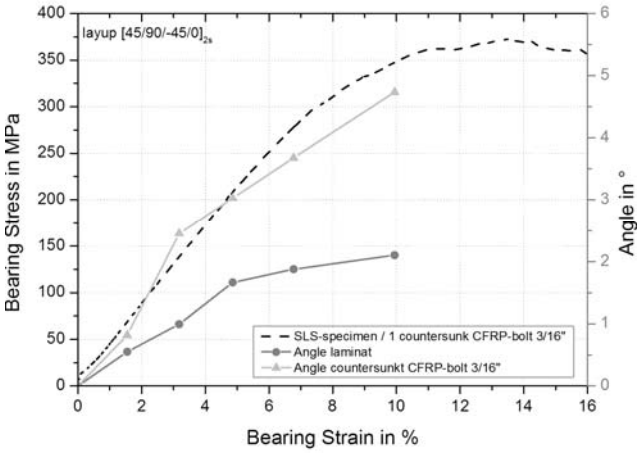

Fig. 6: Bearing Stress/Strain curve for a SLS-specimen with one countersunk CFRP-bolt including the bolt and laminate angle

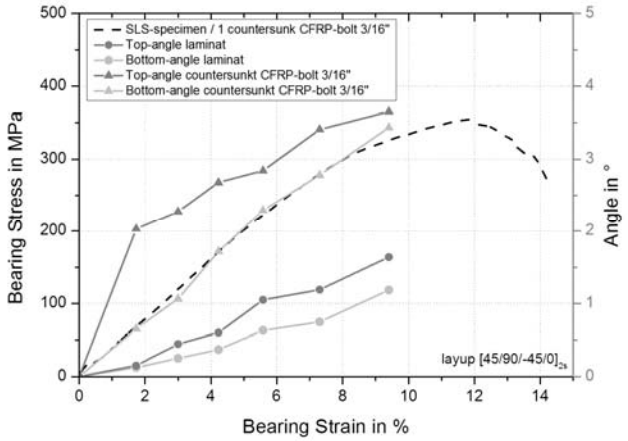

Fig. 7: Bearing Stress/Strain curve for a SLS-specimen with two countersunk CFRP-bolt including the bolt and laminate angle

Differences in the angle change of the bolts for either one CFRP-fastener (Fig. 6) or two CFRP-fasteners (Fig. 7) differ not as much. The angle of the bolts in load direction is for a specimen with two fasteners only 0.5° smaller than for specimens with one fastener. These results show that for specimens with two fasteners an interaction between two CFRP-bolts has to take place.
In order to monitor the interaction between the two CFRP-bolts during a quasi-static SLS-test, the strain between the two bolts is measured (Fig. 8).

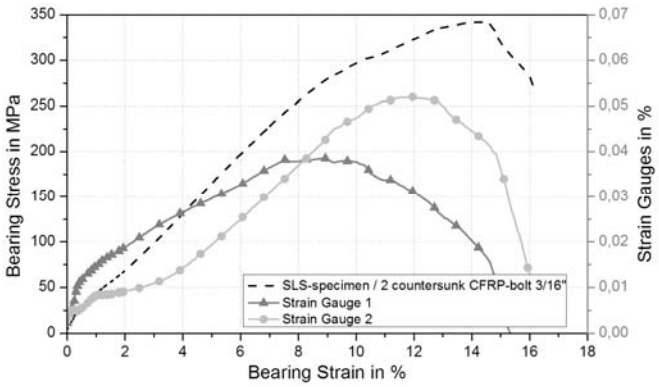

Fig. 8: Bearing stress/strain curve including the strain measured between the bolts

Fig. 8 puts forward the increase of strain between the two fasteners at the beginning of the SLS test. In progress of the experiment the strain reached a maximum, than decreases to zero. The decline of the strain starts close to 10% of bearing strain, where the countersunk heads of the CFRP-bolts start to shear of.

To gain more information about the reaction forces in the bolt due to the loading process, the strain of the bolt during a SLS-test is measured. The bolt strain is plotted against the bearing strain of the SLS-Specimen (Fig. 9).

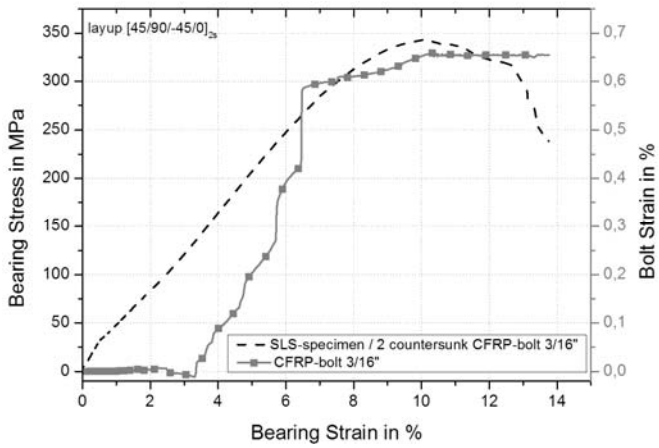

Fig. 9: Bearing stress and bolt strain plotted against the bearing strain for a SLS-Specimen with 2 countersunk CFRP-bolts

The strain of the fastener is calculated by the deformation of the bolt, divided by the initial length of the bolt after the mounting process. The initial length for the measured bolt elongation in Fig. 9 was determined with $l_0 = 22.05$ mm.

Fig. 9 exemplifies the bolt strain during one quasi-static SLS-test. It can be observed that during the beginning of the experiment no elongation of the bolt can be detected. After the test specimen reaches a global bearing strain of 3 %, a rapid gain of bolt strain is detected. Upon further loading at a bearing strain of 10 % no significant elongation of the fastener can be detected. The maximum bolt strain is 0.65 %.

Comparing these results with the information for the bolt and plate angle and the strain measurement between the bolts, it can be seen that at $\varepsilon^{br} = 10\%$ a shear failure in the countersunk head of the CFRP-bolt is detected. In further SLS-tests a measurement of the bolt elongation was not possible above 10 % of bearing strain, due to the fractures in the countersunk head.

In order to study the damage development of the failure process for the CFRP-bolts, fractographic technique is used. With the acoustic emission setup the important steps of the failure process are monitored. In Fig. 10 a typical AE-Signal pattern along with the bearing stress/strain curve of a SLS-test is shown.

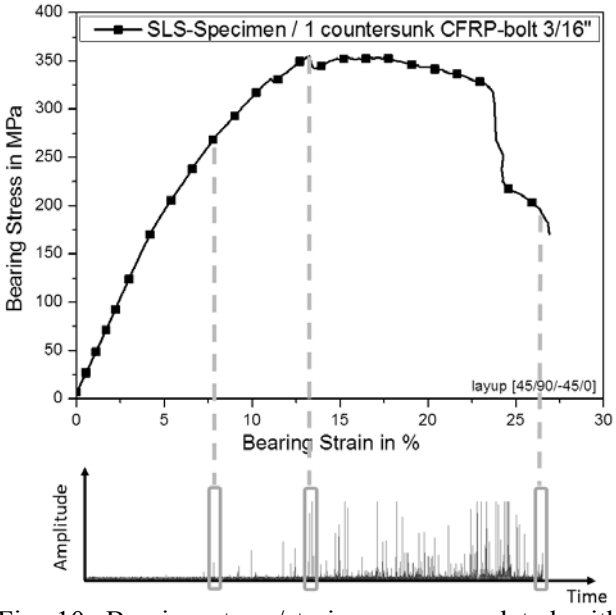

Fig. 10: Bearing stress/strain curve correlated with the AE-signal detected while the SLS-test

The AE-signal is plotted with its amplitude versus time. A correlation of the AE-signal and the bearing stress/strain curve is realised with the elapsed time of the SLS-test. The investigations on the failure process of the CFRP-bolts are mainly performed with specimens with one fastener. So it is possible to focus with the AE-measurement setup on the AE-signals of one bolt. In Fig. 10, three selected events help to describe the failure process of the CFRP-bolt most significantly. They are marked with a box. For each event a SLS-specimen is loaded in tension until the event occurs in the AE-signal. Subsequent to the test, microscopic scans are prepared in 0° cuts to the load direction through the centre of the bolts.
Fig. 11 shows the optical microscopy image of the cut view for the first AE-event under investigation. In the enlarged image section, the middle section of the thread of the CFRP-bolt is shown. The tip of the thread (which consists mainly of matrix) is fractured. Damages to the bolt and nut itself due to the mounting process can be excluded. Cut views in the cross-section taken after assembly of the SLS-specimen show no such failure mechanisms.

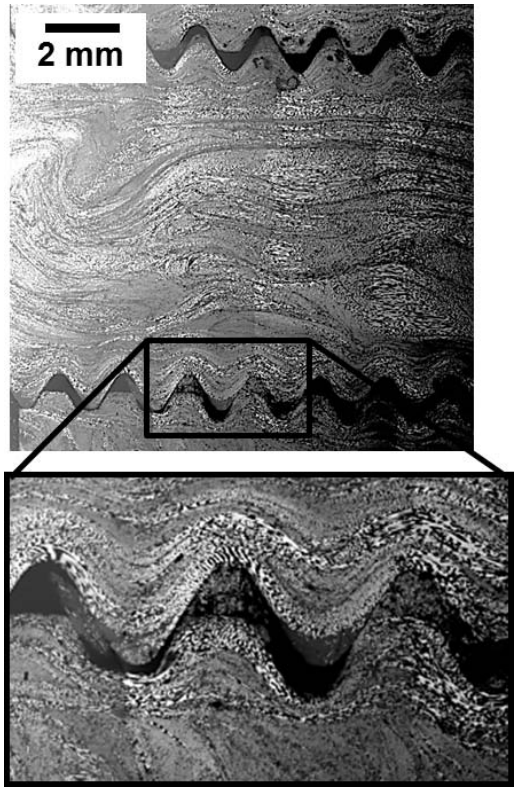

Fig. 11: Optical microscopy cut view of the thread from a CFRP-bolt for the first investigated AE-event

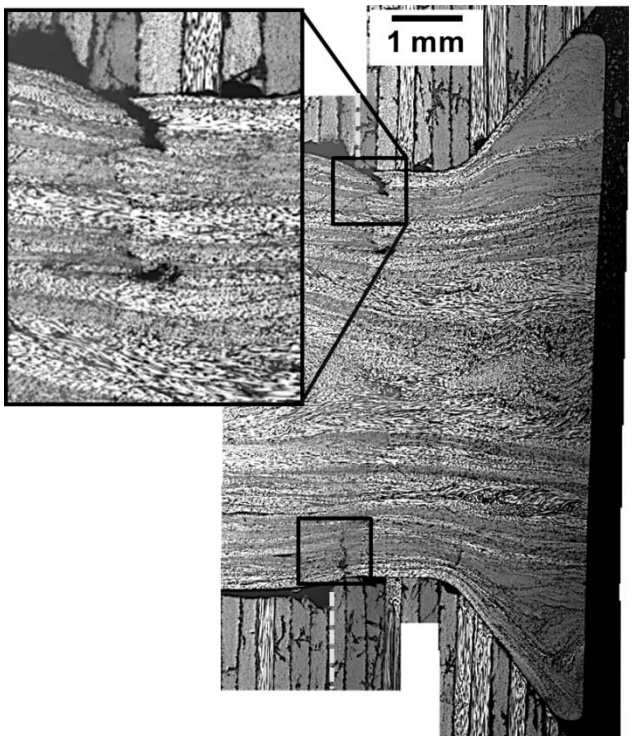

Fig. 12: Optical microscopy cut view of the CFRP-bolt for the second investigated AE-event

Fig. 12 displays the next step in the failure process for the CFRP-bolts is displayed in Fig. 12. Here a damage of the CFRP-bolt in the contact area of the two laminate-plates can be observed. Fibre fractures occur in regions where fibres run perpendicular to the load direction. The contact area is marked in Fig. 12 with a dashed line. A damage of the laminate-plates cannot be detected. Furthermore the countersunk head is complete intact.

Fig. 13 and Fig 14 show the optical microscopy scan of the final failure state for a CFRP-fastener mounted in the laminate plates. During the SLS-test the two laminate plates induce shear and tension force into the bolt. For the failure of the CFRP-bolt three different failure modes can be observed. First inter fibre failures occur in the contact area with the laminate-plates (Fig. 14 (I)), then the countersunk head of the bolt starts to shear of (see Fig. 14 (II)). At last, starting from the tooth flank after the first pitch, inter fibre fractures can be observed as a third failure mode (see Fig. 14 (III)). The development of the crack corresponds to the results observed during a tension test performed to determine the material properties of the CFRP-bolt.

The finale failure of the bolt is due to fibre fracture in the plane of the contact area of the two laminate-plates.
The main failure modes of the laminate plates can be seen in the Fig. 14 (I) and (II). Beside crushed fibres and small delaminations also chip outs at the hole edges of the plates are to be detected.
Investigations for the SLS-test with specimens jointed with two CFRP-fasteners show the same failure mechanisms.
The different failure mechanisms occur due to a combined load case of shear and tension on the CFRP-bolt. The shear forces on the bolt are introduced from the beginning of the test trough the laminate plates. In progress of a SLS-test, the laminate starts to bend under a certain angle. This results in additional tension forces on the CFRP-fastener. Within the range of 8 to 10% of bearing strain the maximum load capacity of the CFRP-joint is reached.

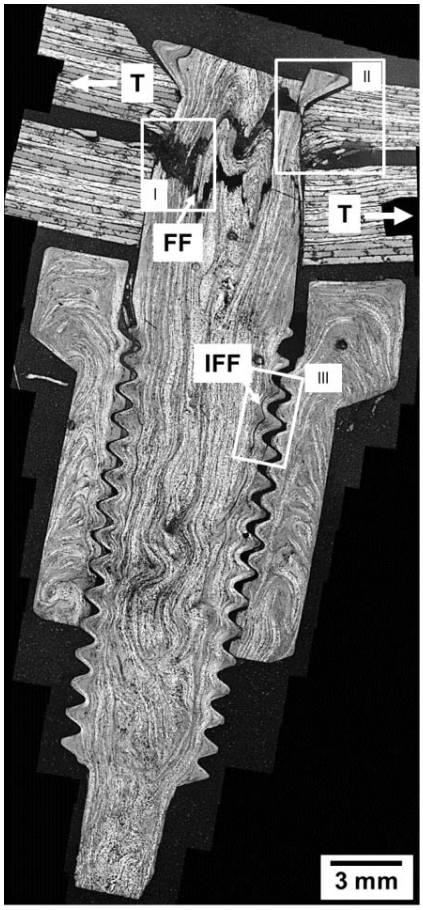

Fig. 13: Optical microscopy cut view of a failed CFRP-bolt inside a SLS-specimen

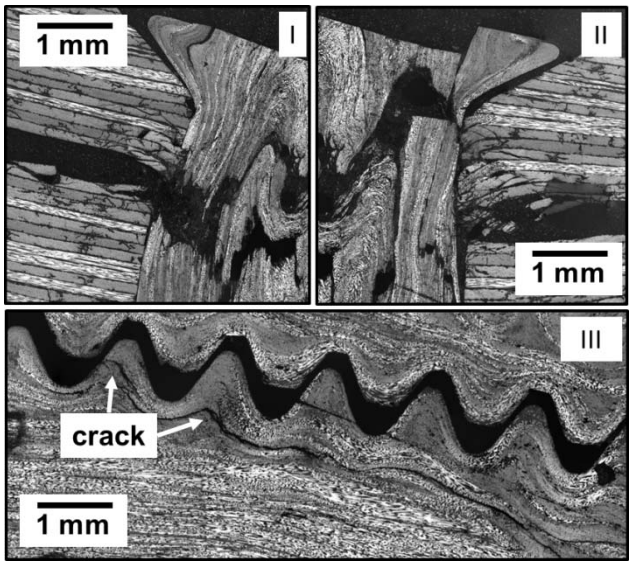

Fig. 14 Optical microscopy cut view of a failed CFRP-bolt inside a SLS-specimen: (I) fibre failure in the bolt shaft, (II) shear failure of the countersunk head, (III) inter fibre fraction in the thread

4 Conclusions

This paper presents an investigation of the failure process for a SLS-test in quasi-static tensile loading. Based on the investigations, several conclusions can be summarized for the failure mechanisms of the CFRP-fastener as follows:

- The Bearing Strength σ^{br} for a SLS specimen with CFRP-bolt is approximately half of that as for a specimen with Ti-bolt.
- The bearing chord stiffness E^{br} of the specimens with CFRP-bolts is equal to 2/3 of the E^{br} of the specimens with Ti-bolts References
- Up to a bearing strain of 10% an increase of the plate and bolt angle, the strain between the two bolts and an elongation of the bolt is detected.
- Between 8 and 10% of bearing strain, the maximum load capacity of the CFRP-bolts is reached and a start of the failure process for the CFRP-bolt is detected.
- During a SLS-test the first detected failures occurred in the thread. The failure could just be seen in the highly resinous areas of the thread.

- First fibre fractures and inter fibre fractures are observed at a bearing strain of 8% in the shaft of the CFRP- bolt.
- Shear of the countersunk head and fibre failures perpendicular in the CFRP-bolt are the observed final failure mechanisms.
- A combined load case of shear and tension on the CFRP-fastener lead to the finale failure of the SLS-specimens.

Further test especially with different parameter configurations will be performed in quasistatic and fatigue loading to see their influence on the joint.
In cooperation with Bishop GmbH Aeronautical Engineers a 3D-Model in ABAQUS is setup, to help understanding the behavior of the bolt in detail. Our aim is to develop a new design of the bolt which can also match with the titanium bolts in maximum stresses.

5 References

[1] H. Schürmann "Konstruieren mit Faser-Kunststoff-Verbunden". First edition, Springer-Verlag Berlin Heidelberg, 2005.

[2] R. Starikov and J. Schön "Quasi-static behaviour of composite joints with countersunk composite and metal fasteners". Composites Part B, 32, pp. 401-411, 2001.

[3] R. Starikov and J. Schön "Fatigue resistance of composite joints with countersunk composite an metal fasteners". International Journal of Fatigue 24, pp. 39-47, 2002.

[4] R. Starikov and J. Schön "Local fatigue behaviour of CFRP bolted joints". Composites Science and Technology 62 24, pp. 243-253, 2002.

[5] W.S. Johnson "Optimization of Joints in light weight composite structurs" *ECCM15* Venice, Italy, 2012

[6] C. Stocchi, P. Robinson, S.T. Pinho "A detailed finit element investigation of composite bolted joints with countersunk fasteners". *ICCM18*, Jeju Island, Korea, 2011.

[7] R. Gutkin, C.J. Grenn, S. Vangrattanachai, S.T. Pinho, P.T. Curtis "On acoustic emission for failure in CFRP: Pattern recognition and peak frequency analyses". Mechanical Systems and Signal Processing 25, pp. 1393-1407, 2011.

[8] P.A. Smith, K.J. Pascoe, C. Polak, D. O. Stroud "The behaviour of Single-lap Bolted Joints in CFRP Laminates" Composite Structures 6, pp 41-55, 1986

[9] T. Ireman " Three-dimensional stress analysis of bolted single-lap composite joints" Composite Structurs 43, pp 195-216, 1998

[10] R.R. Tofnini "Das Composite-Fliesspressen: Ein neues Verfahren zur Net-Shape Fertigung von Endlosfaserverstärkten Bauteilen mit thermoplastischen Matrix dargestellt am Beispiel einer Schraube für Translaminare Wirbelfixation" Dissertaion ETH Nr. 14112, 2001

[11] ASTM D 5961/D 5961M-01 „ Standard Test Method for Bearing Response of Polymer Matrix Composite Lamiantes" ASTM International, 2003